

Design of a 34-GHz Second-Harmonic Coaxial Gyroklystron Experiment for Accelerator Applications

Melany R. Arjona and Wes G. Lawson, *Senior Member, IEEE*

Abstract—In this paper, we present the complete design of a 34-GHz, four-cavity coaxial gyrokystron experiment. The 500-kV, 300-A beam is produced by a double anode magnetron injection gun (MIG) with an average perpendicular-to-parallel velocity ratio of 1.5 and a parallel velocity spread of less than 5%. The microwave circuit has a first-harmonic TE_{011} input cavity that is driven at 17.135 GHz. It has buncher, penultimate, and output cavities that operate in the TE_{021} -mode and are resonant near the second harmonic of the gyrofrequency. A peak power of 55 MW is obtained with a 47-dB gain and 36.5% efficiency. A complete description of the system is presented. We also present scaled circuit designs at 17 GHz and 91 GHz.

Index Terms—Gyrotrons, high-power amplifiers, RF sources.

I. INTRODUCTION

THE range in frequencies near 34 GHz is currently of great interest for many applications, including radars and linear accelerators. The current design of the next linear collider with a center-of-mass energy of 0.5–1 TeV uses 11.424 GHz, 50–75 MW klystrons [1]. Because of average power considerations for linear colliders with center-of-mass energies above 1 TeV, current tentative scenarios anticipate that RF source frequencies will have to be increased to somewhere between Ka-Band and W-Band [2].

At the University of Maryland, we have a program to develop high-power gyrotron amplifiers for electron-positron collider applications. Over the past decade, we have designed, constructed, and tested several dozen gyrokystron and gyrotwystron amplifier tubes ranging in frequencies from X-Band to Ka-Band [3]. Furthermore, we have performed system designs as high as 95 GHz [4]. We are currently testing an experimental second-harmonic, three-cavity tube that is predicted to produce peak powers above 100 MW at 17.136 GHz [5]. For the design presented in this paper, we started by scaling this Ku-Band system to 34.272 GHz. Both the electron gun and the microwave circuit were scaled. The scaled design served as a starting point on which significant reoptimization was performed before arriving at the system described below. Details of the magnetron injection gun (MIG) design are presented in Section II. The microwave circuit design is discussed

Manuscript received October 11, 1999; revised December 1, 1999. This work was supported by the US Department of Energy, Division of High-Energy Physics.

The authors are with the Department of Electrical and Computer Engineering and Institute for Plasma Research, University of Maryland, MD 20742 USA (e-mail: eng.umd.edu).

Publisher Item Identifier S 0093-3813(00)05702-7.

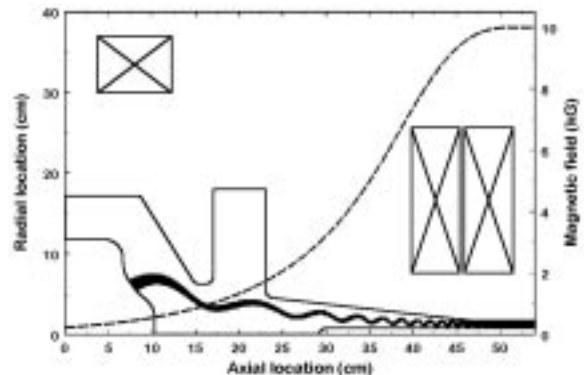


Fig. 1. The Magnetron Injection Gun configuration and simulated beam trajectory.

in Section III. In Section IV, we discuss the scaling of these results to other frequencies of interest.

II. MAGNETRON INJECTION GUN

The MIG layout is shown in Fig. 1. Eight coils were used to generate the magnetic field, including a bucking coil that is centered over the emitter. The gun design is based on the single-anode MIG for the 17-GHz tube [3]. A scaling code was used to obtain the starting dimensions [6]. After being scaled, the design was changed by adding a control anode and by changing the boundaries in both anodes and the cathode until the required parameters were obtained with the minimum velocity spread. A beam optics code called *EGUN* [7] was used to simulate the performance of the electron gun. Details of the design process are given elsewhere [4]. It is sufficient to say that many iterations of the simulations were performed with different numbers of rays and different mesh sizes to ensure that the results were reasonably well converged. For the results of Fig. 2, we were using 47 rays and 20 meshes/cm.

The simulated trajectory is also indicated in Fig. 1. The parameters of the gun and the results of the design simulation at the nominal beam parameters are summarized in Table I. The beam voltage is the same as for the Ku-Band tube, but the nominal current is only 50% of the 17-GHz system value. The necessity of the control anode was dictated by the scaling equations and the requirement on beam current. The control anode voltage required to produce the proper average velocity ratio of $\alpha = 1.5$ is 43% of the full beam voltage. The magnetic compression ratio is fairly conservative at about 22. At 5.7 A/cm², the cathode

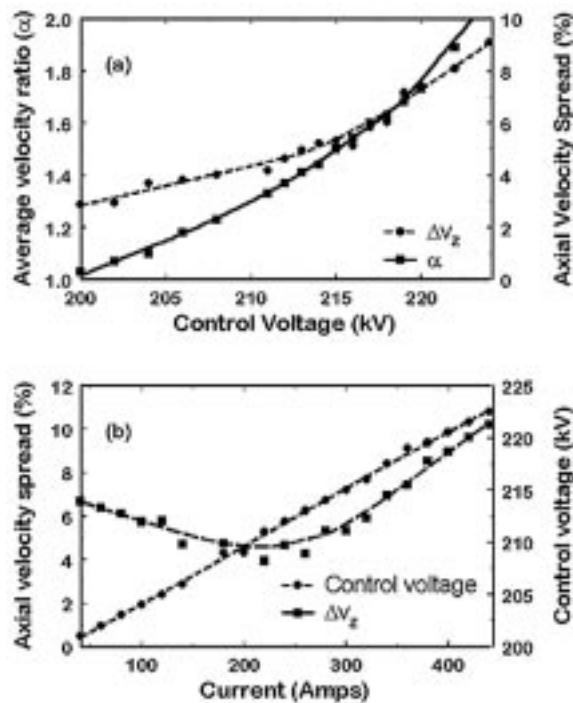


Fig. 2. The simulated beam performance: (a) the dependence of velocity ratio on control anode voltage, and (b) the dependence of velocity spread on beam current.

TABLE I
ELECTRON GUN SPECIFICATIONS AND SIMULATED PERFORMANCE

Beam voltage (kV)	500
Beam current (A)	300
Cathode radius (cm)	6.03
Emitter width (cm)	1.36
Emitter angle (deg)	53
Cathode loading (A/cm^2)	5.71
Cathode magnetic field (kG)	10.10
Control anode voltage (kV)	214.7
Average velocity ratio	1.5
Axial velocity spread (%)	4.84
Average beam radius (cm)	1.27
Peak cathode field (kV/cm)	80
Peak anode field (kV/cm)	69
Peak control anode field (kV/cm)	62
Space-charge current (A)	600

loading is well within the state-of-the-art. The electric field is also reasonably conservative at less than 80 kV/cm everywhere. The average cathode radius is only about 80% of the size of the 17-GHz MIG. With an average cathode angle of 53° and a curved emitter, the beam produced by this MIG is laminar throughout the acceleration region and only begins to mix near the end of the magnetic compression region.

In Fig. 2, we plot two standard parametric dependencies for the MIG. As can be seen from Fig. 2(a), a range of ± 14 kV in the control voltage will change the average velocity ratio from one to two. As expected, increasing the velocity ratio increases the axial velocity spread. At $\alpha = 2$, the axial velocity spread is still below 10%. The dependence of axial velocity spread on beam current is shown in Fig. 2(b). The required change in the

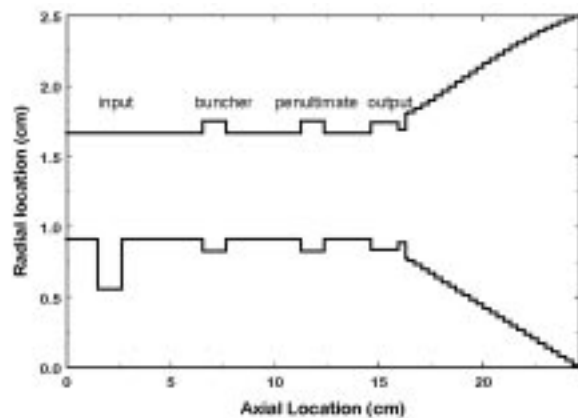


Fig. 3. The layout of the four cavity coaxial gyroklystron circuit.

control anode voltage to keep α at 1.5 throughout this range in currents is indicated by the circles in the figure. The required voltage change is proportional to the current change and has a total swing of ± 11 kV. The minimal spread is actually below the design current at about 250 A. The laminar beam helps keep the spread sufficiently low to be useful over a wide range in currents. Note that above 300 A, the dependence of spread on current is approximately linear and that the spread remains below 10% up to 400 A.

III. MICROWAVE CIRCUIT

A picture of the circuit layout is shown in Fig. 3. Our coaxial amplifier circuit is made of input, buncher, penultimate, and output cavities that are connected by drift regions. The inner conductor is necessary to force the drift regions to be cutoff to the operating modes and, therefore, isolate the cavities from each other. In recent experiments, the inner conductor has been supported by two tungsten pins in the drift region that are intercepted by the beam. However, we have a design of an inner conductor that is supported in the collector region. The amplifier simulation results are not affected by the details of the inner conductor support system, so we will just assume the configuration shown in the figure. The input cavity interacts at the first harmonic in the TE_{011} -mode; all other cavities interact near the second harmonic in the TE_{021} -mode. The nominal drive frequency is 17.135 GHz. Simulations showed that a buncher cavity was necessary to dramatically increase the gain and power of the tube. Also, a detuned penultimate cavity was necessary to further improve efficiency. The input, buncher, penultimate, and output cavities are stagger-tuned to increase efficiency and bandwidth. Their cold resonant frequencies are 17.136 GHz, 34.269 GHz, 34.203 GHz, and 34.255 GHz, respectively.

The starting parameters for the circuit came from scaling the input, buncher, and output cavities from the 17-GHz design and adding the penultimate cavity. The inner conductor forces the TE_{01} -mode to be cutoff at 17 GHz and the TE_{02} -mode at 34 GHz in the drift regions, thereby substantially isolating the cavities. The radial transitions on the inner and outer walls of the second-harmonic cavities are equalized to minimize mode conversion from the TE_{02} - to the TE_{01} -mode. This is required be-

TABLE II
MICROWAVE CIRCUIT PARAMETERS AND SIMULATED RESULTS

Input Cavity	
Radius (cm)	1.663
Inner radius (cm)	0.553
Length (cm)	1.148
Input drive power (kW)	1.03
Buncher Cavity	
Maximum radius (cm)	1.749
Inner radius (cm)	0.826
Length (cm)	1.111
Penultimate Cavity	
Radius (cm)	1.750
Inner radius (cm)	0.825
Length (cm)	1.111
Output Cavity	
Main section radius (cm)	1.742
Inner radius (cm)	0.833
Length (cm)	1.323
Amplifier performance	
Power (MW)	55.2
Efficiency (%)	36.8
Gain (dB)	47.3

cause the TE_{01} -mode is not cutoff in the drift regions at 34 GHz. The output cavity has a diffractive lip to achieve the required Q . The inner conductor is linearly tapered to zero after the output cavity, because it is no longer necessary. The outer waveguide radius has a smooth nonlinear taper to minimize mode conversion. (The steps in the output waveguide seen in Fig. 3 are for simulation purposes only.) The simulated mode purity is over 99.5% for the TE_{02} -mode.

The details of the design procedure are described elsewhere [4]. Basically, the scaled cavity dimensions were adjusted to optimize the tube performance. The simulation code *COAX* is a scattering matrix code that is used to adjust the cavity dimensions to get the proper resonant frequencies of each cavity and the proper Q of the output cavity [8]. To assure stability, another code was used: *QPB* [9]. This code gives the Q (for each cavity) below which the device will be stable as a function of magnetic field and beam power and has been shown to be in good agreement with experiment and other codes [10]. Once we had a viable circuit, *MAGYKL* was run to obtain the system efficiency [11]. *MAGYKL* has been compared with experimental results for other gyrokystrons at the Naval Research Laboratory and the University of Maryland and has always given good agreement [10], [12], [13]. *MAGYKL* has been modified for this effort to automatically optimize for applied magnetic field and drive frequency and power. Numerical checks were made on *MAGYKL* by varying the number of particles used to model the beam. The cycle of using *COAX*, *QPB*, and *MAGYKL* to design the circuit is iterated until an optimal configuration is identified.

The dimensions of the microwave circuit and the simulated results from *MAGYKL* are given in Table II. The system was found to work best at a flat magnetic field of 10.10 kG with an input power of 1.03 kW. The optimal results for the simulated beam parameters include a gain and efficiency of 47 dB and

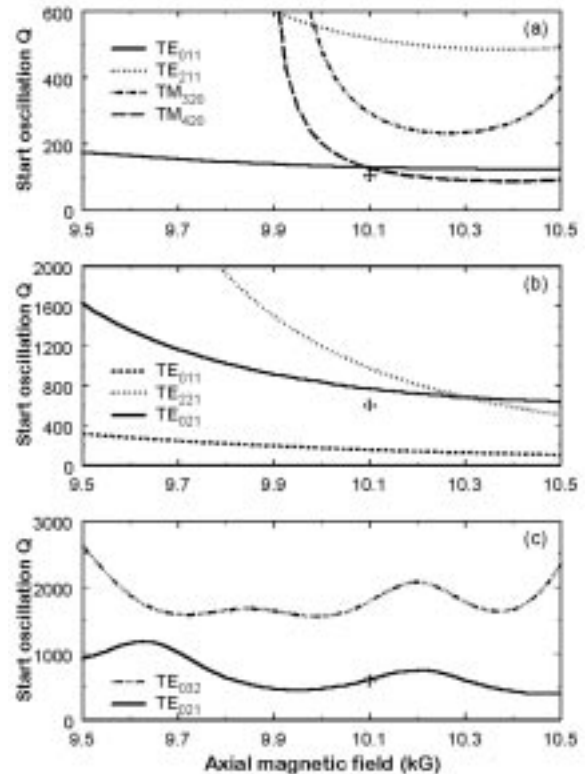


Fig. 4. Start oscillation thresholds for the (a) input, (b) buncher, and (c) output cavities. The crosses indicate the Q of the operating mode and the magnetic field in each cavity.

36.8%, respectively, which translates to an output power of over 55 MW.

The start oscillation curves are shown in Fig. 4. Because of the similarity between penultimate and buncher cavities, only one of them is plotted. The design operating Q 's for the input, buncher, penultimate, and output cavities are approximately 105, 600, 600, and 600, respectively. These numbers were chosen for all but the output cavity to be 80% of the corresponding threshold start Q for each cavity at the nominal operating magnetic field. The output cavity is run just below the start oscillation threshold to maximize efficiency.

Other modes with relatively low start Q 's are also plotted in Fig. 4. Modes in these complex cavities are not pure; they are identified in the graphs by the component that has the largest amplitude in the cavity. The Q 's of the modes in the output cavity are essentially diffractive and known to be stable from the simulations. The Q 's in the buncher and penultimate cavities typically come from resistive loss and are not known from our simulations, which assume perfect conductors. The input cavity mode Q 's are a combination of diffractive and resistive losses and therefore are also not known exactly. However, from previous cold test and numerical simulations that include loss, we believe that all of our cavities are stable at the operating point. Specifically, this includes the TE_{011} -mode for the buncher cavity shown in Fig. 4(b), because the construction techniques we use typically result in a TE_{011} Q , which is about an order of magnitude below the TE_{021} Q [14].

After the design was finalized, some systematic studies were performed. In the following paragraphs, we will present the be-

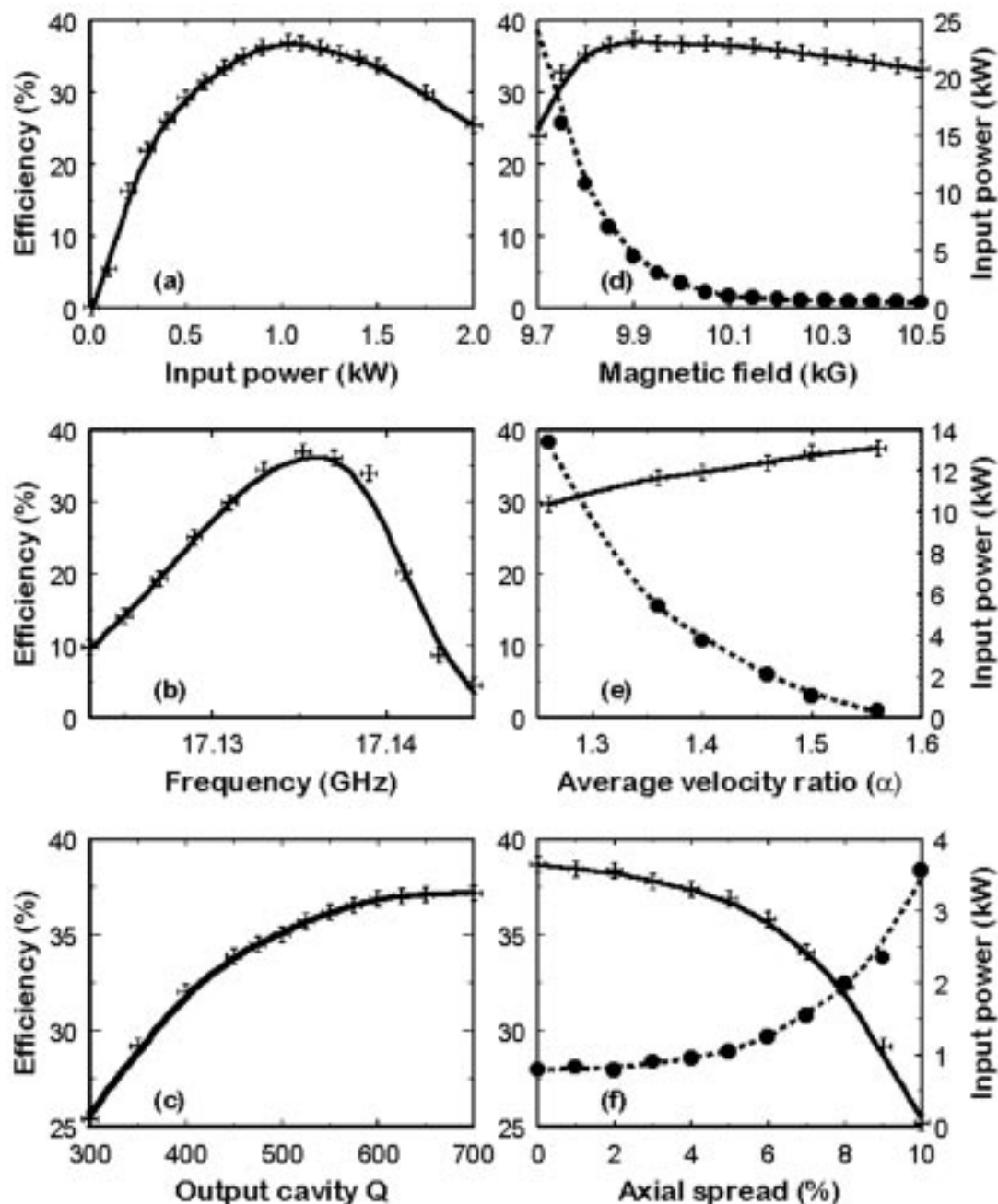


Fig. 5. Parametric study of the microwave circuit. The dependence of efficiency on (a) input power, (b) drive frequency, (c) output cavity quality factor, (d) magnetic field, (e) average velocity ratio, and (f) axial velocity spread. For curves (a) and (b), all other system parameters are held constant. For curves (c)–(f), the drive power was adjusted to maximize the efficiency. The resultant input power is indicated in (d)–(f) by the circles. The drive power in (c) was essentially constant.

havior of our system as a function of some key parameters. In each of the figures, only one or two parameters are varied and the remaining parameters are fixed at the optimal values. The crosses always indicate the simulated efficiency. When a second parameter is varied, it is always the input power and it is indicated by the circles.

Fig. 5(a), we show the drive curve for the tube at the optimal system parameters. As advertised, the system is optimized at an input power of 1.03 kW and an efficiency of 36.8%. The figure clearly shows that the tube is zero-drive stable. The small signal gain is about 51 dB. The efficiency as a function of frequency is shown in Fig. 5(b). The bandwidth was found to be about 0.09%.

This value corresponds to a little more than $1/(2Q_{\text{output}})$ and is consistent with the results for other second-harmonic tubes. These results were obtained at the optimal input power of 1.03 kW; a considerably larger bandwidth could be achieved if the drive power was varied. The dependence of efficiency on output cavity quality factor is plotted in Fig. 5(c). The output cavity Q could be increased to achieve higher efficiencies (but only by less than 1%), but the operating point would exceed the start oscillation Q and the system would become zero-drive unstable.

The dependence of efficiency on magnetic field is plotted in Fig. 5(d). As we can see from the figure, the efficiency is not highly dependent on magnetic field above the optimal point.

However, the efficiency and gain decay quickly as the magnetic field decreases below the optimal point. In Fig. 5(e), we show the dependence of efficiency on velocity ratio and the input power required to optimize every point. If α is increased, the efficiency increases slightly as well to a maximum of 37.4% at an α of 1.56 and an input power of 304 W. However, the output cavity is zero-drive unstable at this point. Finally, in Fig. 5(f), we plot the relationship between efficiency and velocity spread as computed by MAGYKL and the input power required to optimize each point. Our MIG is predicted to produce a beam with 4.84% spread. We can see from the figure that the efficiency for an ideal beam (zero spread) is 38.7%. Note that our design's efficiency is about 2% lower than that of the ideal beam and that the efficiency remains above 30% for velocity spreads up to about 9%.

IV. DESIGN SCALING

There are two components to the system design scaling with frequency: the MIG and the microwave circuit. There are many possible approaches to scaling the design. We take an approach that is consistent with the MIG scaling discussed in [6]. If limits on magnetic compression have not been reached, we can find a scaled MIG design where the beam current is proportional to the wavelength. If the beam voltage is held constant, the beam power is also proportional to wavelength.

Because the scaling of MIG's with frequency has been thoroughly discussed, we concentrate here on scaling the circuit parameters, given the beam power scaling discussed in the previous paragraph. To scale the resonant frequencies of the cavities, all dimensions must be scaled with wavelength. The guiding center radius and the cyclotron orbit (i.e., the gyroradius and axial periodicity) also scale with wavelength, so all drift tube dimensions will scale with wavelength as well. To keep the gain and efficiency constant, we need to keep the cavities at the same relative points on the start-oscillation curves. Because the product of the quality factor and the beam power is a constant, the quality factor must be inversely proportional to the wavelength. This arrangement will result in a constant gain, so the drive power must be proportional to the wavelength.

One or two modifications to the circuit dimension scaling are dictated by this Q scaling. First, if the output cavity Q is determined by a diffractive lip, the lip dimensions (e.g., the lip length) will have to be adjusted to achieve the necessary Q . This is true because the diffractive Q is unchanged by frequency scaling. Because the quality factors scale with frequency, the relative bandwidth of the tube scales proportionally with the wavelength. Furthermore, if stagger tuning is employed in the original design, the relative frequency shifts in the scaled tube need to be adjusted in accordance with the Q 's. This can usually be easily achieved with slight modifications to the cavity wall radii. If the bandwidth scaling is not acceptable, cavity lengths can be adjusted to compensate, but that will also affect the system gain and efficiency.

We have scaled the 34-GHz circuit to 17 GHz and to 91 GHz, according to the formulation described above. The key parameters in each design are contrasted in Table III. The precise scaling resulted in efficiencies above 34% in both cases.

TABLE III
A COMPARISON OF THE SCALED TUBE PERFORMANCE

Parameter	17 GHz Design	34 GHz Design	91 GHz Design
Circuit Magnetic field (kG)	5.05	10.1	26.93
Total tube length (cm)	50.976	25.593	9.652
Input Cavity: f (GHz) / Q	8.568/ 53	17.136 / 105	45.695/ 280
Buncher Cavity: f (GHz) / Q	17.134/ 300	34.269 / 600	91.386/ 1600
Penultimate Cavity: f (GHz) / Q	17.068/ 300	34.203 / 600	91.320/ 1600
Output Cavity: f (GHz) / Q	17.120/ 300	34.255 / 600	91.372/ 1600
Drive frequency (GHz)	8.568	17.135	45.693
Gain (dB)	47.8	47.3	48.3
Efficiency (%)	35.2	36.8	36.6
Output Power (MW)	105.5	55.2	20.6

Small adjustments in the peak power brought the Ku-Band and W-Band tube efficiencies up to 35.2% and 36.6%, respectively. The efficiencies are close, as would be expected because the designs are scaled from the Ka-Band result. They are not identical because the stagger tuning is different for each case because of the change in the relative bandwidth. Further enhancements in efficiency could probably be achieved by making minor modifications to the other circuit parameters.

V. SUMMARY

The four-cavity gyrokystron design presented in this paper is predicted to produce 55 MW of peak power at 34.27 GHz. This high power is obtained from the interaction between a second-harmonic output cavity and a 300-A, 500-kV beam that is produced by a double-anode MIG. According to simulations, the high-quality beam will facilitate an interaction efficiency of 36.8% with a high gain (47 dB). The tube is predicted to be zero-drive stable. A design procedure for scaling gyrokystron circuits over wide-frequency ranges was presented. Scaled circuits at 17 GHz and 91 GHz were modeled with the MAGYKL code and were predicted to produce peak powers of 105 MW and 20 MW, respectively, with efficiencies comparable to the 34-GHz design.

REFERENCES

- [1] T. O. Raubenheimer *et al.*, "Zeroth order design report for the next linear collider," Stanford, CA, SLAC Rep. SLAC-R-0474, May 1996.
- [2] P. B. Wilson, "Scaling linear colliders to 5 TeV and above," Stanford, CA, SLAC Rep. SLAC-PUB-7449, Apr. 1997.
- [3] V. L. Granatstein and W. Lawson, "Gyro-amplifiers as candidate RF drivers for TeV linear colliders," *IEEE Trans. Plasma Sci.*, vol. 24, pp. 648-665, 1996.
- [4] M. R. Arjona and W. Lawson, "Design of a 7 MW, 95 GHz, three-cavity gyrokystron," *IEEE Trans. Plasma Sci.*, vol. 27, pp. 438-444, 1999.
- [5] G. P. Saraph, W. Lawson, M. Castle, J. Cheng, J. P. Calame, and G. S. Nusinovich, "100-150 MW designs of two and three cavity gyrokystron amplifiers operating at fundamental and second harmonics in X- and Ku-band," *IEEE Trans. Plasma Sci.*, vol. 24, pp. 671-677, 1996.
- [6] W. Lawson, "Magnetron injection gun scaling," *IEEE Trans. Plasma Sci.*, vol. 16, pp. 290-295, 1988.
- [7] W. B. Herrmannsfeldt, "Electron trajectory program," Stanford, CA, SLAC Rep. SLAC-PUB-0331, Oct. 1988.
- [8] W. Lawson and P. E. Latham, "The scattering matrix formulation for overmoded coaxial cavities," *IEEE Trans. Microw. Theory Tech.*, vol. 40, pp. 1973-1977, 1992.
- [9] P. E. Latham, S. M. Miller, and C. D. Striffler, "Use of lie transforms to generalize mady's theorem for computing gain in microwave devices," *Phys. Rev. A*, vol. 45, pp. 1197-1206, 1992.

- [10] M. Blank *et al.*, "Experimental investigation of W-band (93 GHz) gyrokystron amplifiers," *IEEE Trans. Plasma Sci.*, vol. 26, pp. 409–415, 1998.
- [11] P. E. Latham, W. Lawson, and V. Irwin, "The design of a 100 MW, Ku-band, second harmonic experiment," *IEEE Trans. Plasma Sci.*, vol. 22, pp. 804–817, 1994.
- [12] W. Lawson *et al.*, "Efficient operation of a high-power X-band gyrokystron," *Phys. Rev. Lett.*, vol. 67, pp. 520–523, 1991.
- [13] —, "High-power operation of a three-cavity X-band coaxial gyrokystron," *Phys. Rev. Lett.*, vol. 81, pp. 3030–3033, 1998.
- [14] M. Castle, J. Anderson, W. Lawson, and G. P. Saraph, "An overmoded coaxial buncher cavity for a 100 MW gyrokystron," *IEEE Microw. Guided Wave Lett.*, vol. 8, pp. 302–304, 1998.



Melany R. Arjona was born in Panama City, Panama in 1977. For the past three years she has been working at the Institute for Plasma Research as an Undergraduate Research Assistant while pursuing a B.S. degree in electrical and computer engineering at the University of Maryland at College Park.



Wes G. Lawson (S'84–M'85–SM'97) received the B.S. degree in mathematics (1980) and the B.S. (1980), M.S. (1981), and Ph.D. (1985) degrees in electrical engineering from the University of Maryland. His dissertation work involved theoretical and experimental studies of microwave generation in various large-orbit gyrotron configurations.

Wes worked in the Electric Systems Branch of Harry Diamond Laboratories from 1978 to 1982. He has been with the University of Maryland's Laboratory for Plasma Research for the past 17 years and is currently a Professor in the Department of Electrical Engineering. His principle interest lies in novel fast-wave microwave sources and his recent efforts have been directed toward high power fast-wave and hybrid amplifiers and associated high power microwave components.